Cell Reports
Report

Cell PRESS
Open ACCESS

Long Open Reading Frame Transcripts Escape Nonsense-Mediated mRNA Decay in Yeast

Laurence Decourty,[1] Antonia Doyen,[1] Christophe Malabat,[1] Emmanuel Frachon,[2] Delphine Rispal,[3,4] Bertrand Séraphin,[3] Frank Feuerbach,[1] Alain Jacquier,[1,*] and Cosmin Saveanu[1,*]

[1]Génétique des Interactions Macromoléculaires, Institut Pasteur, CNRS UMR3525, 25-28 rue du docteur Roux, 75015 Paris, France
[2]Production de Protéines Recombinantes et d'Anticorps (PF5), Institut Pasteur, 25-28 rue du docteur Roux, 75015 Paris, France
[3]Equipe Labellisée La Ligue, Institut de Génétique et de Biologie Moléculaire et Cellulaire (IGBMC), INSERM U964/CNRS UMR 7104/Université de Strasbourg, 67404 Illkirch, France
[4]Present address: Department of Molecular Biology, University of Geneva, 30 quai Ernest-Ansermet, 1211, Geneva 4, Switzerland
*Correspondence: alain.jacquier@pasteur.fr (A.J.), cosmin.saveanu@pasteur.fr (C.S.)

http://dx.doi.org/10.1016/j.celrep.2014.01.025

SUMMARY

Nonsense-mediated mRNA decay (NMD) destabilizes eukaryotic transcripts with long 3′ UTRs. To investigate whether other transcript features affect NMD, we generated yeast strains expressing chromosomal-derived mRNAs with 979 different promoter and open reading frame (ORF) regions and with the same long, destabilizing 3′ UTR. We developed a barcode-based DNA microarray strategy to compare the levels of each reporter mRNA in strains with or without active NMD. The size of the coding region had a significant negative effect on NMD efficiency. This effect was not specific to the tested 3′ UTR because two other different NMD reporters became less sensitive to NMD when ORF length was increased. Inefficient NMD was not due to a lack of association of Upf1 to long ORF transcripts. In conclusion, in addition to a long 3′ UTR, short translation length is an important feature of NMD substrates in yeast.

INTRODUCTION

Nonsense-mediated decay (NMD) is a translation-dependent mechanism that leads to degradation of eukaryotic RNAs with long 3′ UTRs (reviewed in Kervestin and Jacobson, 2012). Such transcripts are often described as having a premature termination codon (PTC) and can arise from inefficiently spliced pre-mRNAs that were exported to the cytoplasm (Sayani et al., 2008), RNAs generated through alternative splicing (He et al., 2003; Mendell et al., 2004), or cytoplasmic unstable "noncoding" RNAs (Thompson and Parker, 2007). In contrast to the common assumption that NMD substrates are rare in eukaryotes, recent large-scale transcript analyses have uncovered an important fraction of yeast transcripts that contain short open reading frames (ORFs) in the 5′ UTR of annotated coding sequences (upstream ORFs [uORFs]) (Arribere and Gilbert, 2013; Pelechano et al., 2013). Such uORF-containing transcripts are good substrates for NMD in both yeast (He et al., 2003) and mammals (Hurt et al., 2013).

NMD depends on three major conserved factors: Upf1 (Nam7 in yeast), an ATP-dependent RNA helicase, Upf2 (Nmd2 in yeast), and Upf3, with additional proteins involved in the process in metazoans and possibly in yeast (He and Jacobson, 1995; Luke et al., 2007). Binding of Upf1 to transcripts is correlated with degradation of these transcripts through NMD in yeast (Johansson et al., 2007). It has been recently postulated that Upf1 binding to long 3′ UTR regions could represent the molecular mark that leads to mammalian mRNA degradation through NMD (Hogg and Goff, 2010). Large-scale Upf1 crosslinking to RNA data indicate that although NMD substrates are more likely to be bound by Upf1 (Hurt et al., 2013), Upf1 binds many transcripts not affected by NMD (Zünd et al., 2013). These studies have shown that blocking translation results in a loss of specificity of Upf1 binding to 3′ UTRs. Whether Upf1 is actively recruited on 3′ UTRs during translation termination (Kurosaki and Maquat, 2013; Shigeoka et al., 2012) or is displaced from ORF regions by translation is unclear.

The presence of Upf1 on a long 3′ UTR thus seems required, but not sufficient, for NMD. Additional molecular events, like an aberrant translation termination, are likely to affect the stability of an Upf1-bound mRNA. Results obtained with NMD reporters with PTCs that are far from the poly(A) tail in *S. cerevisiae* (Amrani et al., 2004), *D. melanogaster* (Behm-Ansmant et al., 2007), and mammalian cells (Eberle et al., 2008; Singh et al., 2008) led to the proposal that the long distance between the PTC and the poly(A) tail affects translation termination and thus triggers NMD (Amrani et al., 2004).

Although many studies were focused on the influence of the 3′ region on NMD efficiency, little is known about the influence of the region upstream of the stop codon in the process. To address this issue, and to analyze the importance of the region upstream of the stop codon in NMD, we have set up an experimental system that addresses on a large scale the context in which an otherwise normal termination codon is able to trigger

Cell PRESS
Open ACCESS

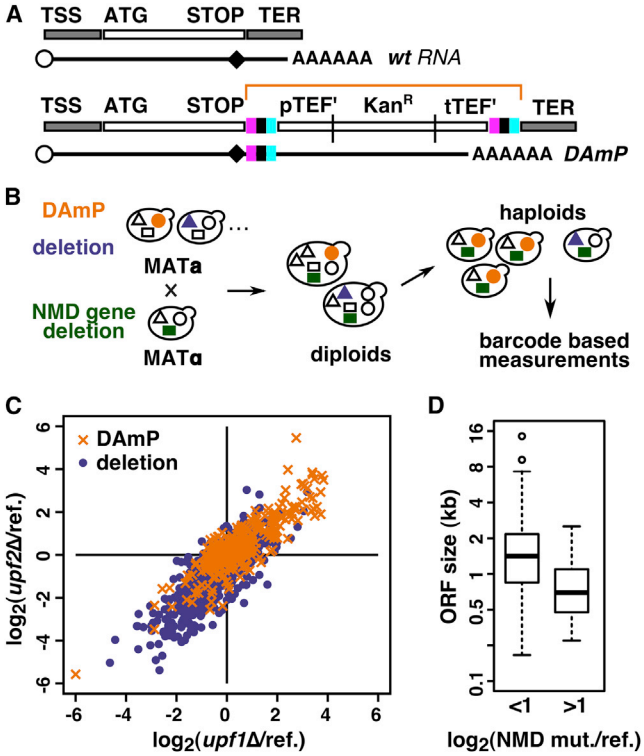

Figure 1. DAmP Modification Preferentially Affects Short Essential Genes Function

(A) Schematics of the DAmP modification. TSS, transcription start site; TER, natural transcription termination region; pTEF′, Kan^R, and TerTEF′ indicate the promoter, G418 resistance ORF, and terminator of the KanMX4 cassette, respectively. Filled black rectangles mark barcode regions flanked by universal priming sequences, whereas a black diamond indicates the ORF stop codon.

(B) Strategy for large-scale analysis of the effect of NMD inactivation on DAmP and gene deletion strains based on the GIM method (Decourty et al., 2008). Filled symbols correspond to gene deletion (blue and green) or DAmP modification (orange) alleles.

(C) Correlation between the effects on growth for deletion and DAmP strains when NMD was inactivated via deletion of either *UPF1* or *UPF2* (n = 4,488, $p < 10^{-16}$, Kendall). Each value is the average of results from two independent screens. Orange crosses correspond to DAmP strains and blue dots correspond to deletion strains.

(D) The DAmP strains showing the strongest growth recovery when combined with NMD inactivation (log_2 value > 1) correspond to genes that have shorter than average ORFs; $p < 3 \times 10^{-12}$, Mann-Whitney U test, n = 744 (less than one category), n = 63 (more than one category).

See also Figure S1.

translation-dependent mRNA decay. This system originates from the observation that lengthening the 3′ UTR destabilizes yeast mRNAs by changing the status of the normal termination codon to a PTC (Muhlrad and Parker, 1999). We studied the steady-state levels of hundreds of mRNAs with an artificial long 3′ UTR expressed from chromosomal-modified genes and their changes in response to NMD inactivation or translation inhibition. These experiments revealed a role for the length of the coding sequence in defining NMD efficiency. These data suggest that the ability of ribosomes to signal a defect in translation termination decreases with longer distances between start and stop codons and reveal short ORF length as a feature of NMD substrates in yeast.

RESULTS

Obtaining and Using a Barcoded Collection of NMD Reporters in Yeast

Replacing natural 3′ UTRs with artificially long sequences allows the generation of strains with altered gene expression that are useful for phenotype or genetic studies of essential genes (decreased abundance by mRNA perturbation [DAmP] strategy; Schuldiner et al., 2005). We have built a collection of 979 DAmP-modified strains (Figures 1A and S1A; Table S1) that can be directly used for large-scale genetic interaction mapping (GIM) screens (Decourty et al., 2008). The DAmP strains that we have generated differ from similar strains reported earlier (Breslow et al., 2008; Yan et al., 2008) because they include molecular barcodes at each modified locus. The locus-specific barcodes situated upstream of the inserted KanMX4 cassette are present in the transcribed DAmP mRNAs, which allows the study of NMD efficiency on hundreds of reporter mRNAs that have the same 1.4-kb-long 3′ UTR yet originate from various promoters and have different 5′ UTR and coding regions.

The GIM method allows one to get a large number of haploid yeast cells that contain two genomic modifications tagged by two different antibiotic resistance markers. The populations of double mutants are then used to investigate quantitative outcomes of combining two mutations in a single cell, which most commonly can lead to a growth rate change. We measured the relative growth rate of 807 DAmP and 3,681 deletion strains (Giaever et al., 2002) inactivated for NMD through deletion of either *UPF1* or *UPF2* as compared with their NMD-competent equivalents (strategy depicted in Figure 1B). Less than 1% of nonessential gene deletion strains displayed an improved growth under these conditions. In contrast, about 8% of DAmP strains showed faster growing rates in combination with NMD mutants (upper right quadrant in Figure 1C; Table S2). This result can be explained by the stabilization of DAmP mRNAs in mutant strains deficient for NMD, followed by increased protein production for the affected gene. We directly tested DAmP mRNA level changes following NMD inactivation in cells expressing the DAmP version of *SMT3*, a strain among those showing a growth improvement when combined with *upf1*Δ or *upf2*Δ (average log_2[NMD inactivation/reference] of 1.9). *UPF1* deletion increased ten times *smt3*-DAmP RNA levels (Figures S1B and S1C). Growth defect suppression by NMD inactivation is thus an indirect indication of the extent of mRNA destabilization elicited by DAmP modification.

The mRNAs most sensitive to the destabilizing effect of a long 3′ UTR, as judged from the growth rate improvement for the corresponding DAmP strains in both *upf1*Δ and *upf2*Δ screens (log_2[NMD inactivation/reference] over 1; Figure 1C) had significantly ($p < 3 \times 10^{-12}$) shorter than average ORFs (Figure 1D). This potential effect of ORF size on NMD efficiency was mirrored by the observation that short gene DAmP strains were more affected for growth than longer gene DAmP strains. A correlation between ORF size and growth defect was not present in the nonessential gene deletion collection (Figure S1D; Table S3).

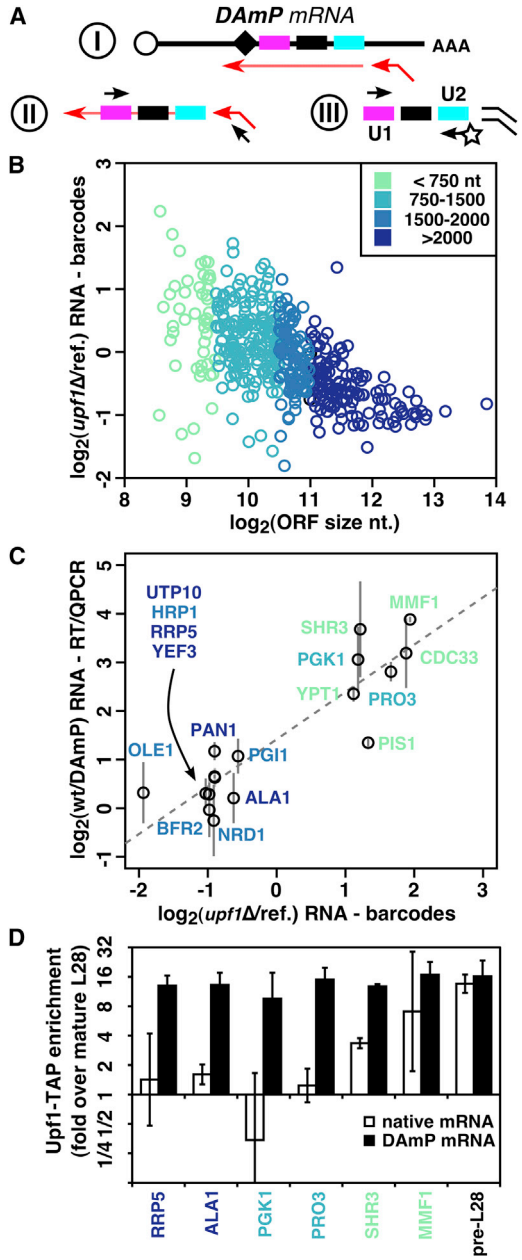

Figure 2. Short ORF DAmP mRNAs Are More Sensitive to NMD Despite Similar Levels of Associated Upf1

(A) The strategy used to measure DAmP mRNA level changes in mixed populations of hundreds of strains consisted of (I) reverse transcription with an oligonucleotide specific to the DAmP cassette, followed by (II) an enrichment PCR and (III) amplification with fluorescent U2 (Cy3 or Cy5) and U1 universal primers. In parallel, DNA samples were used for barcode-region amplification and fluorescent labeling as done for GIM screens. Cyan and magenta rectangles depict universal sequences flanking the barcode region.

(B) Deletions of *UPF1* and *YEL068C* (reference mutation) were added to all the DAmP strains using the mating and sporulation strategy of the GIM method. The increase in the levels of DAmP mRNA in a *upf1*Δ context was inversely correlated with the length of the translated ORF.

(C) The results obtained with the large-scale method were validated by reverse transcription followed by quantitative PCR testing of 17 mRNAs selected from several categories of ORF size. Each DAmP mRNA level was compared with the corresponding mRNA from a wild-type strain. The correlation with the barcode-based results was excellent ($n = 17$, $r = 0.9$, $p < 9.5 \times 10^{-7}$, Pearson). Error bars represent SD based on three independent experiments.

(D) The degree of association for a selection of six DAmP mRNAs to Upf1 was measured in diploid strains expressing Upf1-TAP. The levels of each mRNA (native, white bars; DAmP, black bars) in the purified fraction and in the total cell extract were measured by reverse transcription and quantitative PCR, and fold enrichment was calculated by using mature RPL28 mRNA as control. Unspliced RPL28 pre-mRNA served as a positive control. Error bars represent SD (three independent experiments). A color code based on the size of the corresponding ORFs was used throughout the figure.

See also Figure S2.

A Strategy for Barcode- and GIM-Based Large-Scale Tests of NMD

Although the observed effects on growth indicated a possible link between NMD efficiency and ORF size, we wanted to directly test this effect by measuring the changes in all DAmP mRNA levels when NMD is functional or not. To this end, we developed an experimental strategy that takes advantage of the barcodes specific to each mutant to estimate the levels of DAmP mRNAs in a complex population of strains (depicted in Figure 2A). The barcode-based strategy led to estimates of RNA abundance that were highly correlated ($n = 565$, $r = 0.77$, $p < 2.2 \times 10^{-16}$, Pearson) with published abundance values (Lipson et al., 2009) for the corresponding mRNAs (Figure S2A).

We used the RNA-derived barcode-based method to evaluate the changes in the levels of hundreds of DAmP mRNAs in populations of strains where NMD was inactivated by *UPF1* or *UPF2* deletion (GIM method). *YEL068C* deletion, affecting an intergenic region that has no impact on any known yeast process, was used to generate a reference DAmP population. The strong negative correlation ($n = 470$, $r = -0.57$, $p < 2.2 \times 10^{-16}$, Pearson) observed between the increase in mRNA levels in the absence of Upf1 and the initial ORF size (Figure 2B; Table S4) suggested that ORF size could be a major determinant of NMD efficiency. Because NMD depends on translation, we also evaluated changes in DAmP mRNA levels after blocking translation for 30 min with 50 μg/ml cycloheximide. A significant inverse correlation ($n = 523$, $r = -0.44$, $p < 2.2 \times 10^{-16}$, Pearson) was observed between the size of the affected ORFs and DAmP mRNA accumulation upon translation inhibition (Figure S2B; Table S4).

The results obtained with the barcode-based strategy combined with the presence or absence of NMD factors were strongly correlated with changes in the steady-state levels of a set of 17 different mRNAs in individual strains before and after DAmP modification, which were measured by quantitative PCR (Figure 2C). To test the potential influence of cellular phenotypes that could bias the results on the levels of DAmP mRNAs in haploid strains, we measured the relative levels of DAmP mRNAs in heterozygous diploid strains obtained by batch mating of the DAmP strains with a wild-type BY4742 strain. The DAmP mRNA levels in haploid and diploid cells were strongly correlated ($p < 1.2 \times 10^{-13}$, $r^2 = 0.91$) (Figure S2C). Altogether, these data show that addition of a long 3′ UTR to a yeast mRNA elicits translation-dependent transcript instability by NMD only if the ORF is relatively short, whereas longer ORF mRNAs escape NMD.

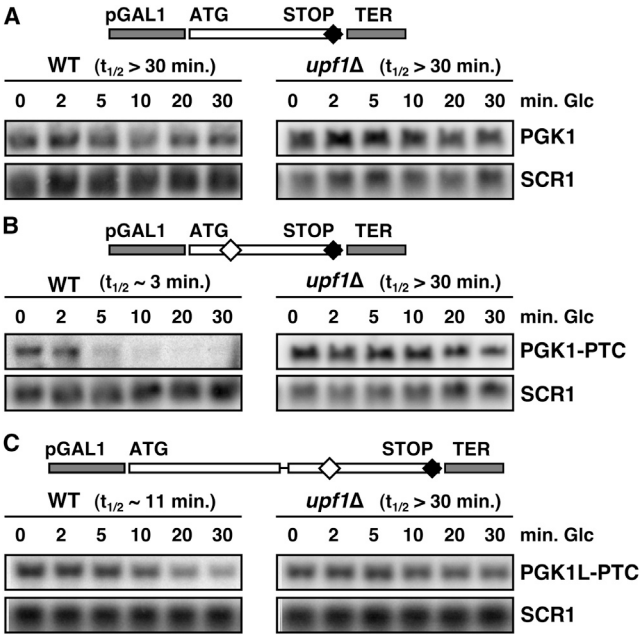

Figure 3. Extending the Translated ORF Decreases NMD Efficiency on a Model Substrate

The stability of *GAL1* promoter-driven *PGK1* reporter mRNA differing in ORF length was tested by transcriptional shutoff and northern blot.

(A) *PGK1* without a PTC had an estimated half-life longer than 30 min.

(B) The insertion of a termination codon 97 nt from start destabilized the mRNA (estimated half-life of 3 min), a situation reversed by *UPF1* deletion.

(C) Increasing the length of the ORF to 1,401 nt by inserting a copy of the *PGK1* ORF upstream of the original PTC-containing PGK1 led to stabilization of the mRNA (estimated half-life of 11 min). Filled and empty diamond symbols indicate stop codons.

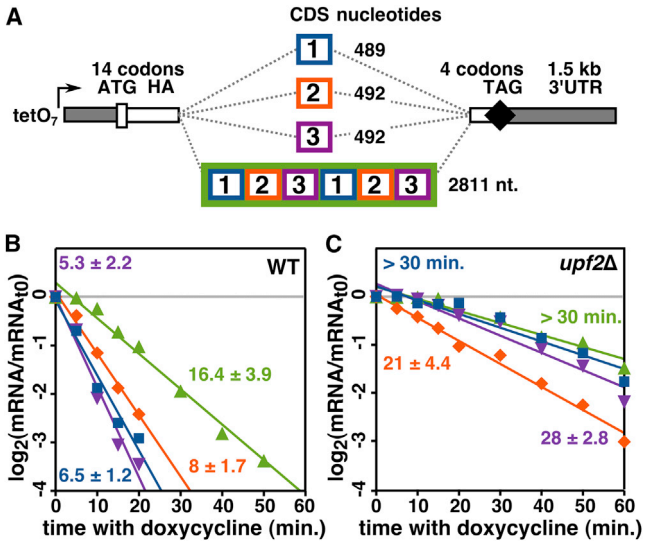

Figure 4. The Size of the Coding Region, Independent of its Sequence, Affects NMD Efficiency

(A) A region of ALA1 coding sequence was cut in three fragments, and each fragment was inserted in a single copy vector allowing expression of mRNAs with a long 3′ UTR under the control of a doxycycline-repressible promoter. A tandem repetition of fragments 1, 2, and 3 was inserted in the same vector.

(B and C) mRNA stability was measured by northern blotting at different time points after doxycycline addition in synthetic complete medium without uracil at 20°C in a wild-type (B) or *upf2*Δ (C) strain. Each decay assay was performed in triplicate, and the median of the results is shown.

See also Figure S4.

The inability of NMD to degrade long-ORF-containing DAmP mRNAs could be due to a decreased association of Upf1 with the transcripts. To test this hypothesis, we affinity purified Upf1-TAP-associated mRNAs from strains expressing DAmP mRNAs and found that the addition of a long 3′ UTR extension to mRNAs with ORFs longer than 2 kb (*RRP5* and *ALA1*) or to mRNAs with ORFs shorter than 1.5 kb (*PGK1*, *PRO3*, *SHR3*, and *MMF1*) led to the same consistent enrichment in association with Upf1 (Figure 2D). Despite the similar association with Upf1, only short ORF DAmP mRNAs (*PRO3*, *SHR3*, and *MMF1*) showed a marked accumulation after a cycloheximide treatment (Figure S2D). The specificity of association of Upf1 with DAmP transcripts decreased after 30 min of treatment with cycloheximide for five of the six DAmP mRNAs tested (Figures S2E and S2F). This result is well correlated with the observed loss of specificity of Upf1 binding to 3′ UTRs when translation is inhibited (Hurt et al., 2013; Zünd et al., 2013). We conclude that Upf1 associates indiscriminately with both long and short ORF mRNAs having a long 3′ UTR extension.

Increasing ORF Length Stabilizes Reporter NMD Substrates

We wondered if the effect we identified with the large-scale study could be observed on typical NMD reporters with a different long 3′ UTR, promoter, and coding sequence. We used the extensively studied *PGK1* reporter system to test the effect of translated ORF size on the stability of a reporter mRNA. Placing an additional copy of *PGK1* ORF upstream and in frame with a *PGK1*-derived reporter bearing a PTC led to stabilization of the corresponding NMD-affected mRNA (Figure 3). The increase in ORF size was accompanied by a decrease in the ratio of coding-sequence length to 3′ UTR length, and we wondered if this ratio could have an influence on NMD efficiency. To test this hypothesis, we measured the steady-state levels of transcripts containing a long ORF (*ADE3*; ORF length 2,841 nt) combined with various 3′ UTR lengths. Only a modest decrease in mRNA levels was elicited by a 1.7 kb 3′ UTR inserted downstream the stop codon of the *ADE3* gene, and this decrease was not enhanced when the 3′ UTR size was increased from 1.7 to 4.8 and 5.9 kb (Figures S3A and S3B). It is thus likely that it is the ORF size and not its ratio compared with the 3′ UTR that plays a role in NMD sensitivity of transcripts.

To establish if ORF size alone, independent of the translated sequence, could affect NMD, we designed a series of NMD reporters consisting of an identical 5′ UTR, start and stop codon context, and a long 3′ UTR. Transcripts containing three different fragments of *ALA1* ORF were tested either alone or in a tandem repeat that created a long coding sequence (Figure 4A). Because mRNA decay for this reporter was too fast to allow precise measurements at 30°C, we measured decay rates of transcripts at

20°C. Increasing the coding sequence length slowed down the NMD-dependent degradation rate of the reporter mRNA (Figures 4B, 4C, and S4B). Because all the sequences contained in the long reporter are translated in one or another of the short transcripts (as verified by western blots; Figure S4C), we concluded that it is ORF size and not the translated sequence that affects NMD efficiency on this reporter. Thus, coding sequence size affected translation-dependent mRNA decay of three different NMD reporters and can potentially affect NMD efficiency on any substrate.

DISCUSSION

Molecular barcodes allow multiplexing of DNA based assays in mixtures of cells or plasmids. We show here that inclusion of barcodes in transcribed sequences also allows parallel tests on hundreds of reporter mRNAs. Barcoded mRNA NMD reporters served to identify short ORF length as an important feature of NMD substrates. Contrary to the model in which Upf1 binding to a long 3′ UTR alone is sufficient to trigger NMD (Hogg and Goff, 2010), our data suggest that ORF size modulates NMD for transcripts associated with Upf1. We do not know yet if the ORF-size effect is due to molecular events affecting translation termination (Amrani et al., 2004) or other steps in the degradation pathway.

The number of ribosomes reaching the termination codon could affect the stability of an Upf1-bound transcript. Ribosome density decreases along the transcripts from initiation to the stop codon (Ingolia et al., 2009), and the ORF length could thus influence the number of translation-termination events. More ribosomes at translation termination could lead, in the presence of a long 3′ UTR, to faster degradation rates. However, we could find no correlation between ribosome density in the 50 nt preceding the stop codon of a given mRNA (Ingolia et al., 2009) and the level of destabilization induced by a long 3′ UTR (not shown). Thus, ribosome density changes along mRNAs are unlikely to explain the ORF-size effect on NMD efficiency. It is possible that it is not the number but the quality of the termination events that is different between long ORF and short ORF transcripts. Inefficient translation termination at early times after translation initiation could allow optimal coupling with the action of NMD factors.

Our observations are consistent with the preference for short ORFs among natural NMD substrates. The bulk of NMD substrates in yeast consists of transcripts that have short ORFs upstream of a long untranslated sequence (Arribere and Gilbert, 2013; He et al., 2003). Abundant mRNAs lack such uORFs (Yun et al., 2012). A paucity of ATG in the 5′ UTR of mRNAs characterizes not only yeast but also many studied organisms (Rogozin et al., 2001). Thus, transcripts with short ORFs (probably mostly uORFs) are likely to be both excellent substrates for degradation, as shown here, and the most prevalent type of NMD substrate in eukaryotes.

EXPERIMENTAL PROCEDURES

The collection of barcoded DAmP strains was built by homologous recombination using PCR products. Oligonucleotide sequences and protocols for analyzing RNA as well as the building strategies for the NMD reporter plasmids are detailed in Supplemental Experimental Procedures.

GIM Screens, Growth Rates, and Double-Mutant Strains

GIM was done as previously described (Decourty et al., 2008), with two exceptions: the barcoded 979 DAmP strains were added to the pool of mutants and a custom-made constant turbidity system for haploids selection and culture was used. This system uses a stream of sterile air that allows continuous culture of yeast in 10 ml reaction flasks. Data analysis of the microarray results was done using R to perform loess normalization with *marray* independently for the UP and DOWN measured sets of ratios (corresponding to the two barcodes situated in the 5′ and 3′ region of the KANMX cassette). Only the measurements coming from at least two independent experiments were further used.

Individual double-mutant strains were obtained by mating and sporulation using the same protocol as the one used in GIM screens. The strains used for GIM screens were obtained from the collection of haploid BY4742-derived strains through replacement of the KANMX4 cassette by a PrMFalpha2-Nat1 cassette, as described elsewhere (Decourty et al., 2008). GIM screens were performed with strains with deletions of *UPF1* (GIM0113), *UPF2* (GIM0461), and *YEL068C* (GIM0139).

mRNA Estimations Based on Barcodes

DAmP strains were generated in such a way that transcription continues over the upstream barcode region and terminates in the TEF′ terminator of the KanMX4 cassette, as estimated from northern blot experiments. To be able to individually measure the level of the DAmP mRNAs in a mixture of more than 900 yeast strains, we performed a three-step labeling protocol (outlined in Figure 2A). First, total RNA was isolated from the pool of DAmP strains without other manipulation or from the pool of double mutants that were obtained through GIM screens done with *upf1*Δ, *upf2*Δ, or *yel068c*Δ. Ten micrograms of RNA were DNase I treated and used in reverse-transcription reactions using an oligonucleotide complementary to a region of the KanMX4 cassette downstream the U2 universal barcode (oligonucleotide CS800; 5′-ATTCAGGGATCCTACCGTCGGCGCGCCTTAATTAACCCG-3′). This oligonucleotide is extended with an artificial sequence that served as a template in a second step of PCR amplification with oligonucleotide U1 (5′-GATGTC CACGAGGTCTCT-3′) and oligonucleotide CS798 (5′-ATTCAGGGATCCT ACCGTCG-3′) and helps to avoid potential cross-contamination with PCR products. The intermediate PCR products obtained in the second step were fluorescently labeled using 5′-labeled Cy3 or Cy5 oligonucleotide U2 (5′-GTCGACCTGCAGCGTACG-3′) and unlabeled U1 oligonucleotide. The final PCR products were hybridized on 8x15k Agilent custom microarrays (Gene Expression Omnibus accession number GPL18088), and R (http://www.cran.r-project.org) was used to filter low signal-to-noise ratios, adjust the median of the $\log_2$-transformed ratios to 0, and calculate average values from two independent reverse-transcription experiments for each tested mutant strain. The differences in cell numbers, when the initial population of cells was coming from GIM screens, were corrected using the formula $(RNA_{mutant}/DNA_{mutant})/(RNA_{ref}/DNA_{ref})$.

ACCESSION NUMBERS

The Gene Expression Omnibus accession number for the data reported in this paper is GSE53954.

SUPPLEMENTAL INFORMATION

Supplemental Information includes Supplemental Experimental Procedures, four figures, and four tables and can be found with this article online at http://dx.doi.org/10.1016/j.celrep.2014.01.025.

ACKNOWLEDGMENTS

We thank Micheline Fromont-Racine and Gwenael Badis-Breard for helpful discussions and criticism, Catherine Gouyette for the synthesis of high-quality oligonucleotides, and Jean-Yves Coppée for access to the GenePix scanner.

Funding was provided by the Institut Pasteur, the CNRS, the CNRS CERBM-IGBMC, the Ligue Contre le Cancer (B.S.; Equipe Labellisée 2011), and the French Agence Nationale de la Recherche (ANR-07- BLAN-0093, ANR-11-BSV8-009-02, and ANR-08-JCJC-0019-01/GENO-GIM).

Received: October 12, 2013
Revised: December 19, 2013
Accepted: January 17, 2014
Published: February 13, 2014

REFERENCES

Amrani, N., Ganesan, R., Kervestin, S., Mangus, D.A., Ghosh, S., and Jacobson, A. (2004). A faux 3′-UTR promotes aberrant termination and triggers nonsense-mediated mRNA decay. Nature *432*, 112–118.

Arribere, J.A., and Gilbert, W.V. (2013). Roles for transcript leaders in translation and mRNA decay revealed by transcript leader sequencing. Genome Res. *23*, 977–987.

Behm-Ansmant, I., Gatfield, D., Rehwinkel, J., Hilgers, V., and Izaurralde, E. (2007). A conserved role for cytoplasmic poly(A)-binding protein 1 (PABPC1) in nonsense-mediated mRNA decay. EMBO J. *26*, 1591–1601.

Breslow, D.K., Cameron, D.M., Collins, S.R., Schuldiner, M., Stewart-Ornstein, J., Newman, H.W., Braun, S., Madhani, H.D., Krogan, N.J., and Weissman, J.S. (2008). A comprehensive strategy enabling high-resolution functional analysis of the yeast genome. Nat. Methods *5*, 711–718.

Decourty, L., Saveanu, C., Zemam, K., Hantraye, F., Frachon, E., Rousselle, J.-C., Fromont-Racine, M., and Jacquier, A. (2008). Linking functionally related genes by sensitive and quantitative characterization of genetic interaction profiles. Proc. Natl. Acad. Sci. USA *105*, 5821–5826.

Eberle, A.B., Stalder, L., Mathys, H., Orozco, R.Z., and Mühlemann, O. (2008). Posttranscriptional gene regulation by spatial rearrangement of the 3′ untranslated region. PLoS Biol. *6*, e92.

Giaever, G., Chu, A.M., Ni, L., Connelly, C., Riles, L., Véronneau, S., Dow, S., Lucau-Danila, A., Anderson, K., André, B., et al. (2002). Functional profiling of the Saccharomyces cerevisiae genome. Nature *418*, 387–391.

He, F., and Jacobson, A. (1995). Identification of a novel component of the nonsense-mediated mRNA decay pathway by use of an interacting protein screen. Genes Dev. *9*, 437–454.

He, F., Li, X., Spatrick, P., Casillo, R., Dong, S., and Jacobson, A. (2003). Genome-wide analysis of mRNAs regulated by the nonsense-mediated and 5′ to 3′ mRNA decay pathways in yeast. Mol. Cell *12*, 1439–1452.

Hogg, J.R., and Goff, S.P. (2010). Upf1 senses 3'UTR length to potentiate mRNA decay. Cell *143*, 379–389.

Hurt, J.A., Robertson, A.D., and Burge, C.B. (2013). Global analyses of UPF1 binding and function reveal expanded scope of nonsense-mediated mRNA decay. Genome Res. *23*, 1636–1650.

Ingolia, N.T., Ghaemmaghami, S., Newman, J.R.S., and Weissman, J.S. (2009). Genome-wide analysis in vivo of translation with nucleotide resolution using ribosome profiling. Science *324*, 218–223.

Johansson, M.J.O., He, F., Spatrick, P., Li, C., and Jacobson, A. (2007). Association of yeast Upf1p with direct substrates of the NMD pathway. Proc. Natl. Acad. Sci. USA *104*, 20872–20877.

Kervestin, S., and Jacobson, A. (2012). NMD: a multifaceted response to premature translational termination. Nat. Rev. Mol. Cell Biol. *13*, 700–712.

Kurosaki, T., and Maquat, L.E. (2013). Rules that govern UPF1 binding to mRNA 3′ UTRs. Proc. Natl. Acad. Sci. USA *110*, 3357–3362.

Lipson, D., Raz, T., Kieu, A., Jones, D.R., Giladi, E., Thayer, E., Thompson, J.F., Letovsky, S., Milos, P., and Causey, M. (2009). Quantification of the yeast transcriptome by single-molecule sequencing. Nat. Biotechnol. *27*, 652–658.

Luke, B., Azzalin, C.M., Hug, N., Deplazes, A., Peter, M., and Lingner, J. (2007). Saccharomyces cerevisiae Ebs1p is a putative ortholog of human Smg7 and promotes nonsense-mediated mRNA decay. Nucleic Acids Res. *35*, 7688–7697.

Mendell, J.T., Sharifi, N.A., Meyers, J.L., Martinez-Murillo, F., and Dietz, H.C. (2004). Nonsense surveillance regulates expression of diverse classes of mammalian transcripts and mutes genomic noise. Nat. Genet. *36*, 1073–1078.

Muhlrad, D., and Parker, R. (1999). Aberrant mRNAs with extended 3′ UTRs are substrates for rapid degradation by mRNA surveillance. RNA *5*, 1299–1307.

Pelechano, V., Wei, W., and Steinmetz, L.M. (2013). Extensive transcriptional heterogeneity revealed by isoform profiling. Nature *497*, 127–131.

Rogozin, I.B., Kochetov, A.V., Kondrashov, F.A., Koonin, E.V., and Milanesi, L. (2001). Presence of ATG triplets in 5′ untranslated regions of eukaryotic cDNAs correlates with a 'weak' context of the start codon. Bioinformatics *17*, 890–900.

Sayani, S., Janis, M., Lee, C.Y., Toesca, I., and Chanfreau, G.F. (2008). Widespread impact of nonsense-mediated mRNA decay on the yeast intronome. Mol. Cell *31*, 360–370.

Schuldiner, M., Collins, S.R., Thompson, N.J., Denic, V., Bhamidipati, A., Punna, T., Ihmels, J., Andrews, B., Boone, C., Greenblatt, J.F., et al. (2005). Exploration of the function and organization of the yeast early secretory pathway through an epistatic miniarray profile. Cell *123*, 507–519.

Shigeoka, T., Kato, S., Kawaichi, M., and Ishida, Y. (2012). Evidence that the Upf1-related molecular motor scans the 3′-UTR to ensure mRNA integrity. Nucleic Acids Res. *40*, 6887–6897.

Singh, G., Rebbapragada, I., and Lykke-Andersen, J. (2008). A competition between stimulators and antagonists of Upf complex recruitment governs human nonsense-mediated mRNA decay. PLoS Biol. *6*, e111.

Thompson, D.M., and Parker, R. (2007). Cytoplasmic decay of intergenic transcripts in Saccharomyces cerevisiae. Mol. Cell. Biol. *27*, 92–101.

Yan, Z., Costanzo, M., Heisler, L.E., Paw, J., Kaper, F., Andrews, B.J., Boone, C., Giaever, G., and Nislow, C. (2008). Yeast Barcoders: a chemogenomic application of a universal donor-strain collection carrying bar-code identifiers. Nat. Methods *5*, 719–725.

Yun, Y., Adesanya, T.M.A., and Mitra, R.D. (2012). A systematic study of gene expression variation at single-nucleotide resolution reveals widespread regulatory roles for uAUGs. Genome Res. *22*, 1089–1097.

Zünd, D., Gruber, A.R., Zavolan, M., and Mühlemann, O. (2013). Translation-dependent displacement of UPF1 from coding sequences causes its enrichment in 3′ UTRs. Nat. Struct. Mol. Biol. *20*, 936–943.